Heavy Seed Survivors in Dwarf Galaxies: A Case Study of Leo I

Matthew T. Scoggins, ^{1*} Zoltán Haiman, ^{1,2,3} and Fabio Pacucci^{4,5} ¹Department of Astronomy, Columbia University, New York, NY, 10027

- ²Department of Physics, Columbia University, New York, NY, 10027
- ³Institute of Science and Technology Austria (ISTA), Am Campus 1, Klosterneuburg, Austria
- ⁴Center for Astrophysics | Harvard & Smithsonian, 60 Garden St, Cambridge, MA 02138, USA
- ⁵Black Hole Initiative, Harvard University, 20 Garden St, Cambridge, MA 02138, USA

Accepted XXX. Received YYY; in original form ZZZ

ABSTRACT

The supermassive black holes (SMBHs) with mass $M_{\bullet} > 10^9 \,\mathrm{M}_{\odot}$ hosted by high-redshift galaxies have challenged our understanding of black hole formation and growth, as several pathways have emerged attempting to explain their existence. The heavy seed explanation eases this problem with the progenitors of these SMBHs having masses up to $\sim 10^5 M_{\odot}$. Here, we investigate the possibility that a local dwarf galaxy, Leo I, holds a heavy seed descendant. Using Monte-Carlo merger trees to generate the merger histories of 1,000 halos similar to the Milky Way (MW), (having a dark matter mass of $\sim 10^{12} M_{\odot}$ at redshift z=0), we search for Leolike satellite halos within these merger trees, and investigate the probability that the minihalo progenitors of these satellites could have formed a heavy seed, or "heavy seed survivors" (HSSs). We investigate the likelihood of formation across various heavy seed formation criteria and Leo-similarity criteria. Of these criteria, we find that the virial temperature that determines the onset of atomic cooling, $T_{\rm act}$, plays a significant role in HSS frequency. We consider three scenarios with decreasing strictness for HSS candidacy, and find an HSS frequency of 0.7%, 18.1%, and 96.5% for T_{act} set to 9, 000K, 7, 000K, and 5, 000K respectively. This suggests that Leo I could be hosting a heavy seed and could provide an opportunity to disentangle heavy seeds from other SMBH formation mechanisms.

Key words: quasars: general – quasars: supermassive black holes – galaxies: active

1 INTRODUCTION

The origin of supermassive black holes (SMBHs) heavier than 10^9 M_{\odot} powering quasars at redshift $z \ge 6$ remains poorly understood (Fan et al. 2001, 2003; Mortlock et al. 2011; Wu et al. 2015; Bañados et al. 2018; Yang et al. 2020; Wang et al. 2021). There are more than 200 detections of these SMBHs (for recent compilations, see Fan et al. (2023) and Bosman (2022)).

The James Webb Space Telescope has recently unveiled a new class of high-z galaxies, named the Little Red Dots (LRDs) (Kocevski et al. 2023; Harikane et al. 2023; Matthee et al. 2023; Kokorev et al. 2024; Maiolino et al. 2024; Baggen et al. 2024; Guia et al. 2024; Kocevski et al. 2025). They are compact high-redshift galaxies thought to host massive black holes, which appear to be overmassive with respect to the local standard relations, suggesting that early black holes got a head start compared to their host galaxies (Pacucci et al. (2023a), but see Li et al. (2025) for a counterargument to this claim).

Understanding high-z black hole formation and evolution requires a new understanding of the mechanisms for rapid and sus-

* E-mail: mts2188@columbia.edu

tained black hole formation and growth. The solutions to this problem typically fall into two categories: 'light' and 'heavy' seeds (Tanaka & Haiman 2009; Volonteri 2010; Inayoshi et al. 2020; Volonteri et al. 2021).

The collapse of gas in primordial dark matter halos is the precursor to the formation of objects in the early universe. This collapse leads to fragmentation, which forms the first stars. For smaller 'minihalos' with virial temperature $T_{\rm vir}$ <10⁴K, this leads to the formation of Population III (Pop III) stars (each with mass of $M\sim10-100\mathrm{M}_{\odot}$) (Abel et al. 2000; Bromm et al. 2001; Abel et al. 2002; Hirano et al. 2014; Katz et al. 2025), which then go on to form 'light' seeds. In some (rare) circumstances, gas inside some minihalos can avoid collapse and grow to the atomic-cooling limit (ACL) where cooling via atomic hydrogen can induce isothermal collapse at $T_{\text{vir}}=10^4 K$, potentially building a supermassive star (SMS) of mass $M \sim 10^3 - 10^5 M_{\odot}$ (Loeb & Rasio 1994; Oh & Haiman 2002; Bromm & Loeb 2003; Lodato & Natarajan 2006; Regan et al. 2020a). If these SMSs formed, they would promptly leave behind 'heavy' black hole seeds. Heavy seeds could also be produced by hyper-Eddington accretion onto a Pop III star black hole remnant (Ryu et al. 2016; Inayoshi et al. 2016) and runaway collisions in dense proto-clusters (Boekholt et al. 2018; Tagawa et al. 2020; Escala 2021; Vergara et al. 2022; Schleicher et al. 2022; Pacucci et al. 2025).

Recent work has focused on developing observational diagnostics. An abnormally high ratio of the luminosity emitted in the He II $\lambda 1640 \text{ vs.}$ the H α line (Tumlinson & Shull 2000; Oh et al. 2001; Johnson et al. 2009, 2010) can diagnose the presence of massive black holes in high-redshift sources. Further, unique spectral signatures in spectral lines and broadband colors (Pacucci et al. 2015, 2016; Nakajima & Maiolino 2022; Inayoshi et al. 2022) and the overmassive black hole relation, where the black hole mass can be comparable or even larger than the total stellar mass, or $M_{\rm bh}/M_* \geq 1$ (Volonteri et al. 2008; Scoggins & Haiman 2024), can distinguish heavy vs. light seeds. This overmassive ratio is several orders of magnitude larger than local black hole to stellar mass relations $M_{\rm BH}/M_* \sim 10^{-3}$ (Reines & Volonteri 2015). The heavy seed pathway may have little or no star formation prior to the formation of the supermassive star (SMS) and subsequent black hole, so this mass ratio could initially, at the birth of the black hole, be as high as 10³. Previous work has focused on estimating the lifetime of this overmassive phase (Scoggins et al. 2022; Scoggins & Haiman 2024), which is expected to decay as the host halo forms stars and/or merges with halos that have a ratio approaching the low-z values. However, this relation may continue to exist in the case of halos that experience very few or no mergers, such as in isolated dwarf galaxies, providing a unique opportunity to search for heavy seed descendants.

A local dwarf galaxy, Leo I, has recently come into focus for this reason. It has been suggested that Leo I could host an unusually massive black hole (Bustamante-Rosell et al. 2021a; Pacucci & Loeb 2022; Pascale et al. 2024, 2025), with recent work suggesting mass $M_{\rm bh} = 3.3 \pm 2.2 \times 10^6 {\rm M}_{\odot}$, and a black hole's existence at 95% confidence (Bustamante-Rosell et al. 2021b). With the total stellar mass estimated to be $M_* = 5.5 \times 10^6 {\rm M}_{\odot}$ (McConnachie 2012), this black hole appears to be overmassive, and may be the descendant of a heavy seed formation site. Pascale et al. (2024, 2025) argue that the black hole mass is lower, few×10⁵ ${\rm M}_{\odot}$, and suggest that Leo I's high DM density can mimic a black hole, and there may be no black hole after all.

Recently, extremely overmassive black holes have also been found a cosmic noon, extending the track of such objects from the epochs probed by JWST (i.e., $z\sim4-10$) towards the local Universe. For example, Mezcua et al. (2024) found 12 SMBHs, which are hosted by low-mass galaxies that are 1-2 orders of magnitude too small, according to local scaling relationships.

Whether Leo I is truly overmassive or even hosts a black hole is an open question. Although the low binding energy of dwarf galaxies makes them more vulnerable to stripping, Leo I appears to have had few mergers in its history. It went through a period of intense star formation but has since run out of gas, and star formation has been mostly quenched (Gallart et al. 1999; Pacucci et al. 2023b). This means that Leo I has had very little change in black hole and stellar mass over Gyr timescales, making it a promising probe of the overmassive relation.

To determine the likelihood of Leo I hosting a heavy seed remnant, we use Monte-Carlo merger trees and a semi-analytic model previously developed in Scoggins & Haiman (2024). We estimate the chance that a heavy seed could end up in a halo similar to Leo I, which we dub 'heavy seed survivor' (HSS). This model estimates the frequency of HSSs in a dwarf galaxy similar to Leo I by searching halos near $z\sim30$ that avoid early fragmentation and reach the atomic cooling limit without prior star formation, where runaway collapse forms a SMS and subsequently a heavy seed.

Applying this model to 1,000 merger trees and tracking halos near redshift z = 0 that share the same properties as Leo I allows us to estimate the fraction of Leo-like satellite halos that could have evolved from a heavy seed hosting galaxy (HSS).

The rest of this paper is organized as follows. In § 2 we describe our methods. In § 3 we present our results. In §4 we discuss these findings. Finally, we summarize our conclusions and the implications of this work in § 5.

2 METHODS

In this section, we summarize the generation of our Monte Carlo dark matter halo merger trees, our heavy seed selection criteria within these merger trees, our selection for Leo-like candidates within these heavy seed hosting branches, and our prescription for stellar mass and black hole growth. This work assumes the following cosmological parameters: $\Omega_{\Lambda}=0.693, \Omega_{m}=0.307, \Omega_{b}=0.0486, \sigma_{8}=0.81$, and h=0.67 (Planck Collaboration et al. 2020).

2.1 Monte-Carlo merger trees

We generate 1,000 Monte-Carlo merger trees for dark-matter halos based on the Extended Press-Schechter theory (Press & Schechter 1974), following the algorithm in Parkinson et al. (2007), which is a modified version of the algorithm used in the GALFORM semi-analytic galaxy formation model (Cole et al. 2000). In order to find Leo-like candidates, we look for satellite halos near a parent halo with a mass and age similar to the Milky Way. This sets the parent mass of our merger tree to $9 \times 10^{11}~M_{\odot}$, at redshift z=0. We set a redshift step size of dz = 0.166, with a minimum mass and mass resolution of $10^5 M_{\odot}$, where star formation is unlikely in halos less massive than this (Kulkarni et al. 2021; Schauer et al. 2021).

2.2 Identifying heavy seed sites and Leo candidacy

Here, we briefly summarize the model of Scoggins & Haiman (2024) that was used in this work. To achieve the intermediary SMS and subsequent heavy seed, H_2 cooling must be suppressed or offset to prevent fragmentation and star formation before reaching the atomic cooling limit. This is achieved through intense Lyman-Werner radiation (with specific intensity J_{LW}) which disassociates H_2 (Haiman et al. 1997; Dijkstra et al. 2008, 2014; Wolcott-Green et al. 2017), dynamical heating via halo mergers (at a rate Γ_{dyn}), and large baryonic streaming motions (ν_{stream}) which can prevent gas infall and contraction. If these processes can prevent fragmentation until the atomic cooling stage with $T_{vir} \sim 10^4 \text{K}$, the emission of atomic hydrogen will rapidly cool the halo, allowing for isothermal collapse, possibly producing a massive BH seed via a SMS.

In order to estimate the influence of these effects, for every snapshot in the merger tree, we calculate the cooling time $t_{\rm cool}$ and compare that to the Hubble time $t_{\rm Hubble}$. Our model for cooling time is dependent on Lyman-Werner radiation and dynamical heating. Here, we briefly summarize the calculation of our halos' Lyman-Werner radiation background and dynamical heating effects, but for the full details see § 2.2 and § 2.3 of Scoggins & Haiman (2024). Following equation (5) of Scoggins & Haiman (2024), we calculate the mean Lyman-Werner radiation expected to be experienced by every halo in our merger trees, $\overline{J}_{\rm LW}(M_{\rm halo},z)$. This captures the mean, but it is expected that the halos that form heavy seeds will experience $J_{\rm LW}$ at the extreme end of the distribution ($J_{\rm LW} \sim 10^3 J_{21}$, e.g. Shang et al. (2010); Glover (2015); Agarwal et al. (2016);

Wolcott-Green et al. (2017)). To account for this distribution for every halo, we draw from a numerically determined J_{LW} distribution shown in Fig. 9 of Lupi et al. (2021), centered on $\overline{J}_{LW}(M_{halo}, z)$. We do this for every halo above the atomic cooling threshold (ACT). For halos just above the ACT, we calculate the ratio $\alpha = J_{LW}/\overline{J}_{LW}$, and the progenitors at and below the ACT are estimated to experience $J_{LW} = \alpha \overline{J}_{LW}$. This accounts for the fact that a halo experiencing unusually high (low) LW flux exists in an overcrowded (underdense) region, and presumably the progenitors of this halo experience a similarly higher (lower) J_{LW} flux. We calculate dynamical heating following equation (1) of Wise et al. (2019),

$$\Gamma_{\rm dyn} = \frac{T_{\rm halo}}{M_{\rm halo}} \frac{k_{\rm B}}{\gamma - 1} \frac{dM_{\rm halo}}{dt},\tag{1}$$

for adiabatic index $\gamma = 5/3$. Using $J_{\rm LW}$, among other details listed in Scoggins & Haiman (2024), to calculate the cooling rate, and Eq. 1 to calculate the heating rate, we can derive an estimate for the cooling time in each halo.

With an estimate for the cooling time for every snapshot, we define two parameters that we will explore in this work: The dimensionless minimum cooling ratio, $\tau_{\rm cool} = t_{\rm cool}/t_{\rm Hubble}$, where snapshots must stay above $\tau_{\rm cool}$ in order to be considered pristine, and the virial temperature of the atomic cooling threshold, $T_{\rm act}$. We consider a halo to be pristine and a direct-collapse black hole (DCBH) candidate at the first snapshot where $T_{\rm vir} \geq T_{\rm act}$. If, for every snapshot before $T_{\rm act}$, the snapshots satisfy $t_{\rm cool}/t_{\rm Hubble} > \tau_{\rm cool}$. After reaching $T_{\rm act}$, it is assumed that runaway atomic cooling condenses the cloud and forms a SMS. For a given $\tau_{\rm cool}$ and $T_{\rm act}$, we find halos that could potentially lead to a heavy seed, and we then follow the subsequent evolution of these halos. We filter these halos for Leo-like candidacy by searching for later snapshots in these branches that meet the following criteria:

- (i) The halo in the merger tree is within the virial mass range of Leo I, $(7 \pm 1) \times 10^8 M_{\odot}$ (Mateo et al. 2008), within one free-fall time of z=0. This results in a window of ~1 Gyr before z=0, or $t_{\rm ff}=\frac{\pi}{2}\frac{d_{\rm Leo}^{1.5}}{\sqrt{2GM_{\rm MW}M_{\rm Leo}}}=1.090$ Gyr for a Leo-MW separation of $d_{\rm Leo}=250$ kpc.
- (ii) The halo has experienced one to three major mergers between z=0.1 and the redshift of the atomic cooling crossing, as suggested by Pacucci et al. (2023b). This introduces another parameter in our search for HSSs, the parameter for what qualifies as a major merger, $q=M_{\rm final}/M_{\rm initial}$. For completeness, we explore the full allowed range of $1 \le q \le 2$.
- (iii) We vary the temperature of the atomic cooling threshold, exploring a range of $T_{\rm act} \in [0.4, 1] \times 10^4 K$.
- (iv) We vary the minimum allowed ratio between the cooling time and the Hubble time for all progenitors before the ACT, $\tau_{\rm cool} = t_{\rm cool}/t_{\rm Hubble}$, exploring $\tau_{\rm cool} \in [0.05, 1]$

Although this version of GALFORM does not explicitly track satellite halos, the Extended Press-Schechter formalism used in this work considers two halos as "merged" when they become closely gravitationally bound. Tanaka & Haiman (2009) has highlighted that for a host halo that is more than 20 times more massive than its satellite, the infall time is so long that the satellite is considered "stuck" and likely never merges. This justifies our choice of searching for Leo-like halos within a free-fall time, although they 'merge' in our merger trees at z=0, they are likely to remain satellites.

We consider a halo to be a Leo-like heavy seed survivor, or HSS, if it meets all of the above criteria. These parameters are summarized in Table 1.

2.3 Stellar Mass painting and black hole growth

We assign stellar masses to our halos following Wise et al. (2014), which finds stellar mass and halo mass statistics from a cosmological simulation. In their Table 1, they provide $\log(M_{\rm vir})$ and $\log(M_*)$ statistics for $6.5 \le \log(M_{\rm vir}/{\rm M}_\odot) \le 8.5$ in 0.5 dex bins. We interpolate across $\log(M_{\rm vir})$ to derive $\log(M_*)$ for a given halo mass and apply this to halos with $10^{6.5} \le M_{\rm halo}/{\rm M}_\odot \le 10^{8.5}$. We note that these statistics are generated from a simulation that ran until z = 7.3, but we apply them to halos with redshift $z \ge 6$.

Black holes are assumed to form shortly after the halos reach the ACT. Similarly to S22, we explore a range of parameters. The initial seed black hole masses in the Renaissance simulation are estimated to fall within the range $10^4 \mathrm{M}_\odot \leq M_{\mathrm{bh}} \leq 10^6 \mathrm{M}_\odot$ where the gravitational collapse to a SMBH is triggered by a relativistic instability. We note that a resimulation of two of the atomic cooling halos in the Renaissance suite found lower SMS masses of $M \approx 10^2 - 10^4 M_\odot$ (Regan et al. 2020b), with higher J_{LW} yielding a higher mass. However, the halos in this resimulation experienced much smaller J_{LW} values ($\sim 10 J_{21}$) than we investigate in this work ($\sim 10^3 J_{21}$), so we expect our seeds to be more massive. We estimate the initial black hole mass to be some fraction of the baryonic material, $M_0 = f_{\mathrm{cap}} \frac{\Omega_b}{\Omega_m} M_{\mathrm{halo}}$, with this fractional cap set to $f_{\mathrm{cap}} = 0.05$. This typically yields black holes with masses $\sim 10^4 \mathrm{M}_\odot$. The growth of these black holes is assumed to follow the Eddington rate

$$\dot{M}_{\rm bh} = \frac{L_{\rm edd}}{\epsilon c^2} = \frac{4\pi G \mu m_{\rm p} M_{\rm bh}}{\sigma_{\rm T} c \epsilon} = \frac{M_{\rm bh}}{\tau_{\rm fold}} \tag{2}$$

with speed of light c, gravitational constant G, mean molecular weight μ (μ ~0.6 for the ionized primordial H + He gas), proton mass $m_{\rm p}$, Thomson cross section $\sigma_{\rm T}$ and radiative efficiency ϵ . This leads to a black hole mass given by $M_{\rm bh}(t)=M_0\exp(t/\tau_{\rm fold})$ with e-folding time $\tau_{\rm fold}=(\sigma_{\rm T}c\epsilon)/(4\pi\mu Gm_{\rm p})\approx 450\epsilon$ Myr. Assuming a radiative efficiency $\epsilon\approx 0.1$, we set $\tau_{\rm fold}=45$ Myr. We additionally quench black hole growth when the mass of the black hole exceeds a prescribed fraction of the baryonic matter in the halo, capping $M_{\rm bh}\leq f_{\rm cap}M_{\rm halo}\Omega_{\rm b}/\Omega_{\rm m}$. To summarize, our simple model governs black hole formation and growth through $f_{\rm cap}$, $\tau_{\rm fold}$, $M_{\rm halo}$, and M_0 (which is determined by $f_{\rm cap}$ and $M_{\rm halo}$). These parameters are summarized in Table 1. We start the growth of our black holes immediately after formation.

3 RESULTS

In Fig. 1, we compare the HSS frequency across the three parameters explored here, $\tau_{\rm cool}$, $T_{\rm act}$, and q. We include six plots, each showing the total number of HSS candidates across two of the three parameters. For a given value along the x and y axes, the left column shows the maximum number of HSSs across the third parameter not shown on the axes. The right column shows the median number of HSSs along this third parameter. We mark the 300%, 100%, 10%, and 1% lines for the expected number of HSSs per tree, shown in black. White space is shown when there is no HSS candidate in our 1,000 merger trees, which means the probability of hosting an HSS for that combination of parameters is $<10^{-3}$.

The top row shows the results across the minimum mass ratio for mergers, q, and the atomic-cooling threshold crossing, $T_{\rm act}$, with the left column showing the maximum value for each pair across $\tau_{\rm cool}$ and the right column showing the median. We find that, in general, decreasing $T_{\rm act}$ increases the frequency of HSSs. This is because a smaller value of $T_{\rm act}$ focuses on an earlier, lower mass

4 M. T. Scoggins et al

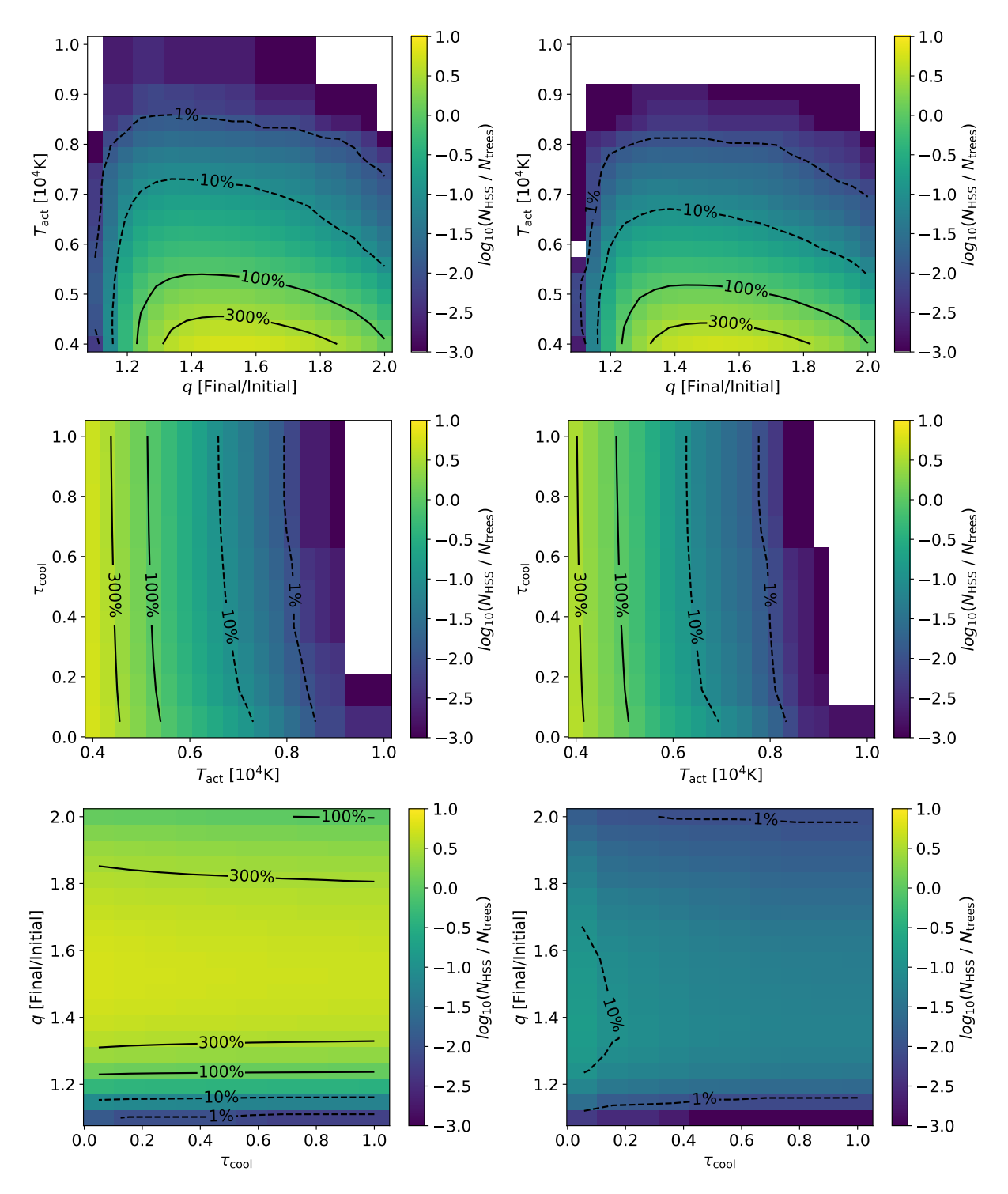


Figure 1. We show $\log_{10}(N_{\rm HSS}/N_{\rm trees})$, the frequency of heavy seed survivors (HSSs), or a Leo-like satellite halo hosting a DCBH descendant, as a function of the criteria that determine HSS candidacy. This criterion includes the halo mass ratio that determines what constitutes a 'major' merger, q, the virial temperature for the onset of atomic cooling, $T_{\rm act}$, and the minimum allowed cooling time ratio, $\tau_{\rm cool} = t_{\rm cool}/t_{\rm Hubble}$. An HSS is formed if, for a $T_{\rm act}$, the halo had avoid any prior star formation (having a cooling time such that $\tau_{\rm cool} > \tau_{\rm cool}$ for every prior snapshot) and the halo experiences one to three 'major' mergers, with mass ratio above q. Each panel explores two of these parameters at a time, with the left column showing the maximum value achieved across the third parameter and the right column showing the median. Lines denote 1%, 10%, 100%, and 300% rates for HSS in our trees. White spaces are shown where there is no HSS in any of our $N_{\rm trees} = 1,000$ merger trees, so the probability of an HSS existing for a given parameter combination is less than 10^{-3} . In some cases, there can be on average three or more HSSs per tree. The HSS frequency has a soft dependence on $\tau_{\rm cool}$, as our halos experience large values of $J_{\rm LW}$ with $\tau_{\rm cool}$ typically greater than 1, so increasing $\tau_{\rm cool}$ does not significantly decrease the number of HSSs. There is a non-linear dependence on q, where a large value of q can result in no mergers, violating the Leo-like criteria, and a small value of q results in too many mergers. The results have a strong dependence on $T_{\rm act}$, as decreasing this value increases HSS rates significantly.

Parameter	Value/Range	Description	
$T_{ m act}$	[4,000,10,000]K	The virial temperature that	
		defines the onset of atomic cooling.	
$ au_{ m cool}$	$t_{\rm cool}/t_{ m Hubble}$	The minimum cooling ra-	
		tio that allows a halo to be considered pristine.	
q	[1.0, 2.0] $M_{\text{final}}/M_{\text{initial}}$	The minimum mass ra-	
		tio that defines a major merger.	
$f_{ m cap}$	0.05	The maximum fraction of baryonic material available	
		for black hole formation and growth.	
$ au_{ m fold}$	45 Myr	Black hole e-folding time.	
M_0	$f_{ m cap} rac{\Omega_b}{\Omega_m} M_{ m halo}$	Initial heavy seed black hole mass.	

Table 1. The values or ranges of several parameters used in this work. These parameters control black hole formation and growth, or control the HSS criteria.

stage in the halo's evolution, reducing the chances for cooling to occur and result in fragmentation. However, the frequency is not monotonic across the minimum mass ratio, and we find that ratios between 1.3 and 1.6 result in the highest HSS occurrence rates. Although a smaller value of q is considered less strict, this tends to result in more mergers than our maximum allowed number of mergers, 3 (we require between 1 and 3 mergers). For the case of $T_{\rm act} \sim 0.4 \times 10^4 {\rm K}$ and $q \sim 1.33$, nearly all of our parent halos host one or more HSS. As $T_{\rm act}$ approaches $0.7 \times 10^4 {\rm K}$, the HSS frequency is 10%, or roughly 100 HSSs in our 1,000 merger trees. For a larger value, $T_{\rm act} \sim 0.9 \times 10^4 {\rm K}$, HSS frequency is less than 1%. The results appear to be similar when comparing the maximum value (left) to the median value (right) across the third parameter, $\tau_{\rm cool}$, signaling that this parameter plays a less significant role in the frequency of HSSs.

The middle rows show the results for $T_{\rm act}$ and $\tau_{\rm cool}$. As expected by the nature of picking the maximum value of $N_{\rm Leo}$, across the third value, q, the results across $T_{\rm act}$ are similar to the top row, with the probability increasing with decreasing $T_{\rm act}$. This explicitly shows that there is little dependence on $\tau_{\rm cool}$, although a lower $\tau_{\rm cool}$ for a fixed $T_{\rm act}$ slightly increases the frequency of HSSs. This weak dependence is likely due to our values of $J_{\rm LW}$ (see Fig. 3 of Scoggins & Haiman 2024), where an abnormally high value that helps the halo remain pristine is usually large enough to keep the cooling time well above $t_{\rm Hubble}$ for the majority of our halos, and a lower value of $\tau_{\rm cool}$ yields little benefit. Again, the results appear to be nearly identical between the left and right panels, where the left explores the maximum across q and the right shows the median across q.

The bottom row explores the HSS frequency across $\tau_{\rm cool}$ and q. On the left, showing the maximum value across $T_{\rm act}$, the majority of the parameter space sees most halos host an HSS, although this maximum value is achieved for an extremely, likely unrealistic, $T_{\rm act}$. Again, there is little dependence on $\tau_{\rm cool}$, the results across q peak near ~ 1.5 . A value of q below 1.2 results in so many 'major' mergers that we regularly exceed our maximum allowed number of three, resulting in almost no HSSs. The right panel, which plots the median HSS number across $T_{\rm act}$, shows an interesting dependence on $\tau_{\rm cool}$ and q, where in this space most of the peak HSS frequency is near $q \sim 1.4$ for an extremely small $\tau_{\rm cool}$. For higher values of $\tau_{\rm cool}$, for the optimal q, the HSS frequency drops to nearly $\sim 30\%$.

Strictness	q	$T_{\rm act}$ [K]	$ au_{ m cool}$
Least	1.4	5,000	0.5
Medium	1.4	7,000	0.75
Most	1.4	9,000	1.0

Table 2. The three cases that define the minimum criteria required in the evolution of a halo in order for it to be considered an HSS.

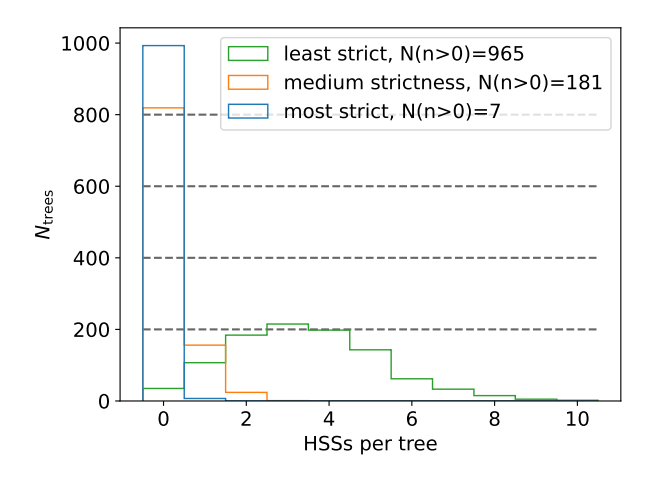


Figure 2. The distribution of the number of HSSs in our 1,000 merger trees. The three cases represent varying degrees of strictness in our three parameters, q, $T_{\rm act}$, and $\tau_{\rm cool}$, with definitions for each case in Table 2. In the least strict case (green), 96.5% of our trees hold at least one HSS, though it is much more common for the trees to have several HSSs. One tree holds as many as 10 HSSs. For the medium case (orange), 18.1% of our trees hold an HSS, with two being the upper limit of HSS per tree. In the strictest case (blue), only 0.7% of our trees have HSSs. This stricter case is the most physically realistic, though future work will be need to put tighter constraints on the specific $T_{\rm act}$ required before atomic cooling kicks in.

Our results for the total number of Leo-like satellite halos that may host a heavy seed, or heavy seed survivors (HSS), for three varying levels of strictness are shown in Fig. 2. Our three cases are defined in Table 2. As the number of HSSs depends nonlinearly on q, we have fixed it to the approximately optimal value of q=1.4, allowing our cases to explore the dependence on the other two parameters. For the least strict scenario (green), the majority of our trees (965 out of 1,000) end up with several HSS candidates, up to 10 HSS in a single tree. For the medium case, 181 out of 1,000 of our trees hold an HSS. Of these, most hold only a single HSS, with a small fraction holding up to two but no more. Finally, in the strictest case, very few HSSs remain. Only 7 of our 1,000 trees have a single HSS. This signals that it is not unreasonable for Leo I to host a heavy seed if this relaxed criterion is practical for heavy seed formation, though there is still hope for even stricter cases.

In Fig. 3 we compare the number of HSSs against $T_{\rm act}$, the most influential parameter for determining how many HSSs end up in a halo. For each merger tree and target $T_{\rm act}$, we take the median number of HSSs across q and $\tau_{\rm cool}$ for that target $T_{\rm act}$. We show the mean (taking the mean across the 1,000 trees, dashed), maximum (solid), and σ (red). This can be thought of as a summary of the information in the top four panels of Fig. 1. For low values of $T_{\rm act}$, we find that there are typically three or more HSSs per tree, but as we approach a more realistic value $T_{\rm act}{\sim}7,000{\rm K}$, there are roughly 50 HSS across the 1,000 trees. Above 9,000K, there are no HSSs. The solid black line shows that the median number of HSSs across

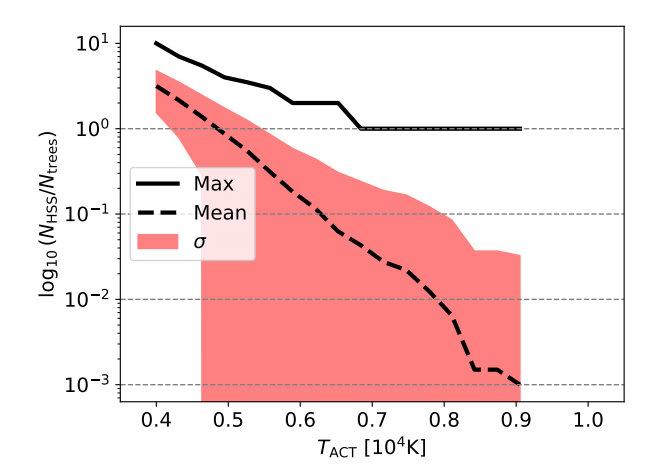


Figure 3. We show HSS frequency as a function of $T_{\rm act}$, the most influential parameter for HSS candidacy. For every tree, we take the median value across q and $\tau_{\rm cool}$ for each target $T_{\rm act}$, then average these results across the trees for our $T_{\rm act}$ range (dashed). We also show the maximum number of HSSs across the 1,000 trees (solid). Red denotes the standard deviation across the 1,000 trees. For low values of $T_{\rm act}$, trees typically hold three HSS, up to a maximum of 10. This frequency declines quickly for increasing $T_{\rm act}$, where there are no HSS for $T_{\rm act} > 9$, 000 Kelvin. The plateau in the maximum number of HSSs signals that from $T_{\rm act} \sim 7$, 000K up to $T_{\rm act} \sim 9$, 000K, there is no more than one HSS in the median value across q and $\tau_{\rm cool}$.

q and $\tau_{\rm cool}$ is 10, though it plateaus to one HSS near $T_{\rm act}$ =7,000K and zero above $T_{\rm act}$ ~9,000K.

In Fig. 4, we show the evolution of our HSS candidate black holes for branches that resulted in HSS candidacy for the least strict case. Although this low $T_{\rm act}$ is unlikely to form a DCBH, as the onset of atomic cooling typically requires $T_{\rm act} \gtrsim 8,000$, the halo evolution is similar in the stricter scenario, and this allows us to see a larger sample size of black holes. In the left panel, we show black hole mass versus redshift, with the median black hole mass shown in black, the standard deviation shown in red, and randomly sampled branches shown in gray. The earliest black hole formation time is near redshift z = 25, with an initial heavy seed mass of $\sim 10^4 M_{\odot}$. The black holes grow to have a median mass of $\sim 4 \times 10^6 \mathrm{M}_{\odot}$ near redshift z=0, which closely matches the mass derived by Bustamante-Rosell et al. (2021b). In the right panel, we show the evolution of our black hole mass against the stellar mass of their host halos. As our black holes grow, they are limited to a fraction of the gas reservoir available in their halo, or 5% of the total baryonic matter. These grow quickly enough that most will soon reach this cap, meaning that halo mass and black hole mass are tightly correlated in this model. We also show stellar mass as a function of halo mass, meaning that the stellar and black hole masses are tightly correlated as well. Near redshift z = 0, most of these satellites have a final BH-to-stellar mass ratio of $M_{\rm bh}/M_*\sim 1$, similar to the ratio observed in Leo I (Pacucci et al. 2023b).

4 DISCUSSION

This investigation hints that the presence of a heavy seed descendant in Leo I, and other similar halos, is plausible under moderately relaxed DCBH formation conditions. While the most restrictive cases only yield $\sim 1\%$ of the MW merger trees as hosting an HSS, the fraction grows rapidly as the conditions are relaxed, yielding 18% and 96% for medium and extremely relaxed conditions. This

suggests that the main uncertainty in HSS frequency lies in the physics of early halo cooling and fragmentation.

The weak dependence on the dimensionless cooling time, $\tau_{\rm cool}$, suggests that halos meeting the heavy seed criteria are typically subjected to intense $J_{\rm LW}$ fluxes, keeping $t_{\rm cool} >> t_{\rm Hubble}$ throughout most of their early evolution and having little influence on HSS frequency. Our mass ratio, $q = M_{\rm final}/M_{\rm initial}$, is used to keep the merger history of our candidates similar to Leo, though this does not constrain dwarf galaxies hosting an HSS in general. The results derived here for a given $\tau_{\rm cool}$ and $T_{\rm act}$ can therefore be thought of as a lower limit for HSS frequency. For Leo-like halos, we find that $q{\sim}1.4$ optimizes HSS frequency, where a large value results in very few or almost no mergers, and a smaller value can result in so many mergers that Leo-like criteria is difficult to achieve.

The dominant parameter in this work is the atomic cooling threshold temperature T_{act} . Decreasing below 9,000K dramatically increases HSS frequency, implying that even small deviations from the canonical 10⁴K threshold can shift the outcome by orders of magnitude. This highlights the importance of follow-up work that investigates non-idealized gas dynamics for the onset of atomic cooling, considering the effects of turbulence, inflows, and anisotropies, which could effectively lower the temperature at which collapse occurs. Some work has suggested that collapse occurs at lower temperatures, near 8,000K (Regan et al. 2020c). Although our lower $T_{\rm act}$ scenarios may appear optimistic, they cannot yet be ruled out. We also note that our calculation for T_{vir} is approximated in this work, where our merger trees only provide the mass and redshift of halos, and we estimate T_{vir} following equation (26) of Barkana & Loeb (2001). The actual gas temperature of a halo given mass $M_{\rm halo}$ at redshift z will vary halo to halo. Furthermore, the gas temperature, which is the truly relevant parameter, is not necessarily equal to $T_{\rm vir}$, and the relationship and scatter between these two have not been fully investigated for atomic cooling halos. See Shang et al. (2010) for further discussion on this point. In our work, for HSSs to not be exceedingly rare, we need atomic cooling to set in near $T_{\rm act}$ ~7,000K, and given the uncertainties discussed above, we can expect that to occur for some unknown fraction of the halos. Future work will need to clarify the scatter in T_{vir} for a given mass and redshift, as well as the relationship between T_{vir} and gas temperature inside of a halo.

If Leo I indeed hosts a ~10⁶M_☉ black hole, its current BHstellar mass ratio is consistent with our evolved HSS predictions, $M_{\rm BH}/M_{*}\sim 1$. The long quenching timescale (Gallart et al. 1999) and lack of mergers (Pacucci et al. 2023b) likely froze its mass ratio near the initial overmassive state, as we have found the ratio to slightly decrease but at a significantly slower rate than is typical for most DCBHs (Scoggins et al. 2022; Scoggins & Haiman 2024). This supports the possibility that Leo I, and dwarf galaxies in general, are excellent testing grounds for $M_{\rm BH}/M_*$ relations. After completing the analysis for this work, another local dwarf galaxy, Segue 1, was recently modeled as having an extremely overmassive black hole (Lujan et al. 2025). The black hole is estimated to have mass $4.5 \pm 1.5 \times 10^5 M_{\odot}$ and comparably very little stellar mass, $M_* \sim 10^3$ (Geha et al. 2009). This results in a BH to stellar mass ratio of $M_{\rm BH}/M_{*}\sim10^{2}$. Future work using either simulations or observational data targeting dwarf systems with similar overmassive ratios at low redshift could directly test this heavy seed scenario.

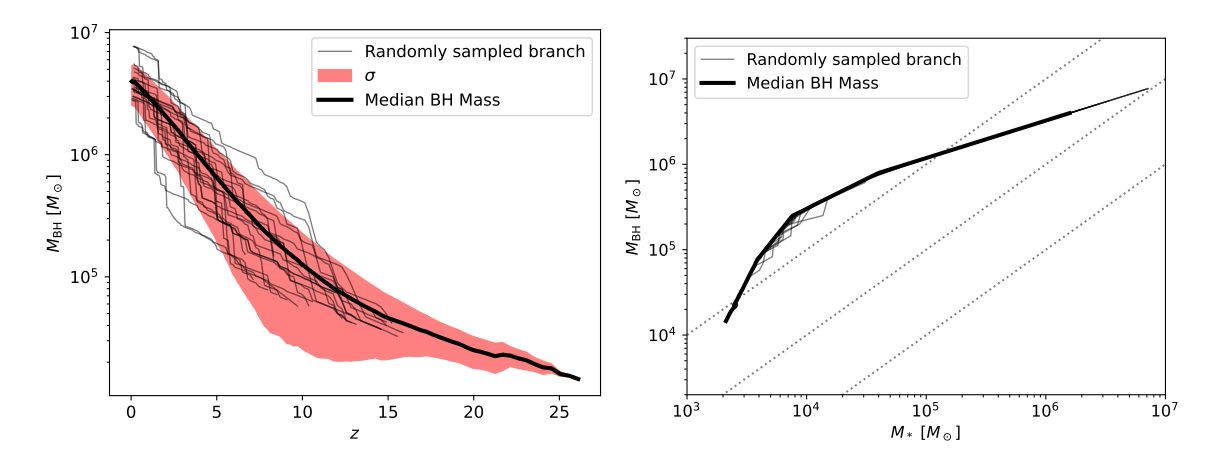


Figure 4. *Left:* The evolution of our HSSs. We show the median black hole mass (black), a few randomly sampled branches (gray) and the black hole mass standard deviation across redshift (red). The median black hole mass terminates in a mass of $\sim 4 \times 10^6 M_{\odot}$, similar to the mass estimated by Bustamante-Rosell et al. (2021b). *Right:* The black hole vs stellar mass for our HSSs. The begin as slightly overmassive, with $M_{\rm BH}/M_* \sim 10$, and terminate with $M_{\rm BH}/M_* \sim 10$.

5 CONCLUSIONS

Dwarf galaxies are thought to be ideal sites to probe potentially preserved $M_{\rm BH}/M_*$ relations from high-z heavy seed sites, with the local dwarf galaxy Leo I being an exciting candidate. This work investigates this possibility by using Monte Carlo merger trees and the model developed in Scoggins & Haiman (2024) to search for 'heavy seed survivors', or DCBH sites that end up in a satellite halo similar to Leo I, orbiting a galaxy similar to the Milky Way. We measure HSS rates as a function of the minimum allowed cooling ratio, $\tau_{\rm cool}$, the temperature that defines the onset of atomic cooling, $T_{\rm act}$, and the minimum merger mass ratio, q.

We find that our results are consistent with Leo I hosting as black hole of mass $\sim 10^6 M_{\odot}$, with a black hole to stellar mass ratio of $M_{\rm BH}/M_*\sim 1$. This suggests that Leo I, and dwarf galaxies similar to Leo I with few major mergers in their history, will preserve the overmassive relation and serve as local probes into high-redshift anxironments.

We find that it is feasible for Leo I to be a descendant of a heavy seed formed at $z \ge 20$, although this possibility is strongly dependent on the exact temperature at which atomic cooling begins, $T_{\rm act}$, and is weakly dependent on q and $\tau_{\rm cool}$. Idealized conditions have set the canonical temperature of $T_{\rm act} = 10^4 {\rm K}$, though recent work has found that this could be lower, closer to 8,000K (Regan et al. 2020c). Future work should aim to refine the details of the onset of atomic cooling, determining the scatter at the specific temperature at which atomic cooling begins, $T_{\rm act}$, as well as the discrepancy between the estimated virial temperature and the temperature at the center of the halo when it begins to collapse.

ACKNOWLEDGEMENTS

ZH acknowledges support from NSF grant AST-2006176. FP acknowledges support from a Clay Fellowship administered by the Smithsonian Astrophysical Observatory. This work was also supported by the Black Hole Initiative at Harvard University, which is funded by grants from the John Templeton Foundation and the Gordon and Betty Moore Foundation. Merger tree generation and analysis were performed with NSF's XSEDE allocation AST-120046 and AST-140041 on the Stampede3 resource. The freely available

plotting library matplotlib (Hunter 2007) was used to construct the plots in this paper.

DATA AVAILABILITY

The code used to analyze the merger trees and generate figures for this manuscript is available at this github repository. All other data will be shared on reasonable request to the corresponding author.

REFERENCES

```
Abel T., Bryan G. L., Norman M. L., 2000, ApJ, 540, 39
Abel T., Bryan G. L., Norman M. L., 2002, Science, 295, 93
Agarwal B., Smith B., Glover S., Natarajan P., Khochfar S., 2016, MNRAS,
    459, 4209
Bañados E., et al., 2018, Nature, 553, 473
Baggen J. F. W., et al., 2024, ApJ, 977, L13
Barkana R., Loeb A., 2001, Phys. Rep., 349, 125
Boekholt T. C. N., Schleicher D. R. G., Fellhauer M., Klessen R. S., Reinoso
    B., Stutz A. M., Haemmerlé L., 2018, MNRAS, 476, 366
Bosman S. E. I., 2022, Zenodo
Bromm V., Loeb A., 2003, ApJ, 596, 34
Bromm V., Ferrara A., Coppi P., Larson R., 2001, MNRAS, 328, 969
Bustamante-Rosell M. J., Noyola E., Gebhardt K., Fabricius M. H., Mazzalay
    X., Thomas J., Zeimann G., 2021a, ApJ, 921, 107
Bustamante-Rosell M. J., Noyola E., Gebhardt K., Fabricius M. H., Mazzalay
    X., Thomas J., Zeimann G., 2021b, ApJ, 921, 107
Cole S., Lacey C. G., Baugh C. M., Frenk C. S., 2000, MNRAS, 319, 168
Dijkstra M., Haiman Z., Mesinger A., Wyithe J. S. B., 2008, MNRAS, 391,
Dijkstra M., Ferrara A., Mesinger A., 2014, MNRAS, 442, 2036
Escala A., 2021, ApJ, 908, 57
Fan X., et al., 2001, The Astronomical Journal, 122, 2833
Fan X., et al., 2003, The Astronomical Journal, 125, 1649
Fan X., Bañados E., Simcoe R. A., 2023, ARAA, 61, 373
Gallart C., Freedman W. L., Aparicio A., Bertelli G., Chiosi C., 1999, AJ,
Geha M., Willman B., Simon J. D., Strigari L. E., Kirby E. N., Law D. R.,
    Strader J., 2009, ApJ, 692, 1464
Glover S. C. O., 2015, MNRAS, 453, 2901
Guia C. A., Pacucci F., Kocevski D. D., 2024, Research Notes of the Amer-
```

ican Astronomical Society, 8, 207 Haiman Z., Rees M. J., Loeb A., 1997, ApJ, 476, 458 Harikane Y., et al., 2023, arXiv e-prints, p. arXiv:2303.11946

```
Hirano S., Hosokawa T., Yoshida N., Umeda H., Omukai K., Chiaki G.,
    Yorke H. W., 2014, ApJ, 781, 60
Hunter J. D., 2007, Computing in Science & Engineering, 9, 90
Inayoshi K., Haiman Z., Ostriker J. P., 2016, MNRAS, 459, 3738
Inayoshi K., Visbal E., Haiman Z., 2020, Annual Review of Astronomy and
    Astrophysics, 58, 27
Inayoshi K., Onoue M., Sugahara Y., Inoue A. K., Ho L. C., 2022, ApJ, 931,
Johnson J. L., Greif T. H., Bromm V., Klessen R. S., Ippolito J., 2009,
    MNRAS, 399, 37
Johnson J. L., Khochfar S., Greif T. H., Durier F., 2010, MNRAS, 410, 919
Katz O. Z., Redigolo D., Volansky T., 2025, J. Cosmology Astropart. Phys.,
Kocevski D. D., et al., 2023, ApJ, 954, L4
Kocevski D. D., et al., 2025, ApJ, 986, 126
Kokorev V., et al., 2024, ApJ, 968, 38
Kulkarni M., Visbal E., Bryan G. L., 2021, ApJ, 917, 40
Li J., et al., 2025, ApJ, 981, 19
Lodato G., Natarajan P., 2006, MNRAS, 371, 1813
Loeb A., Rasio F. A., 1994, ApJ, 432, 52
Lujan N., et al., 2025, ApJ, 992, L25
Lupi A., Haiman Z., Volonteri M., 2021, MNRAS, 503, 5046
Maiolino R., et al., 2024, A&A, 691, A145
Mateo M., Olszewski E. W., Walker M. G., 2008, ApJ, 675, 201
Matthee J., et al., 2023, arXiv e-prints, p. arXiv:2306.05448
McConnachie A. W., 2012, AJ, 144, 4
Mezcua M., Pacucci F., Suh H., Siudek M., Natarajan P., 2024, ApJ, 966,
   L30
Mortlock D. J., et al., 2011, Nature, 474, 616
Nakajima K., Maiolino R., 2022, arXiv e-prints, p. arXiv:2204.11870
Oh S. P., Haiman Z., 2002, ApJ, 569, 558
Oh S. P., Haiman Z., Rees M. J., 2001, ApJ, 553, 73
Pacucci F., Loeb A., 2022, ApJ, 940, L33
Pacucci F., Ferrara A., Volonteri M., Dubus G., 2015, MNRAS, 454, 3771
Pacucci F., Ferrara A., Grazian A., Fiore F., Giallongo E., Puccetti S., 2016,
    MNRAS, 459, 1432
Pacucci F., Nguyen B., Carniani S., Maiolino R., Fan X., 2023a, arXiv
    e-prints, p. arXiv:2308.12331
Pacucci F., Ni Y., Loeb A., 2023b, ApJ, 956, L37
Pacucci F., Hernquist L., Fujii M., 2025, arXiv e-prints, p. arXiv:2509.02664
Parkinson H., Cole S., Helly J., 2007, MNRAS, 383, 557
Pascale R., Nipoti C., Calura F., Della Croce A., 2024, A&A, 684, L19
Pascale R., Nipoti C., Calura F., Della Croce A., 2025, arXiv e-prints, p.
    arXiv:2506.13847
Planck Collaboration et al., 2020, A&A, 641, A6
Press W. H., Schechter P., 1974, ApJ, 187, 425
Regan J. A., Wise J. H., Woods T. E., Downes T. P., O'Shea B. W., Norman
    M. C., 2020b, The Open Journal of Astrophysics, 3
Regan J. A., Haiman Z., Wise J. H., O'Shea B. W., Norman M. L., 2020a,
    The Open Journal of Astrophysics, 3
Regan J. A., Wise J. H., O'Shea B. W., Norman M. L., 2020c, MNRAS,
    492, 3021
Reines A. E., Volonteri M., 2015, ApJ, 813, 82
Ryu T., Tanaka T. L., Perna R., Haiman Z., 2016, MNRAS, 460, 4122
Schauer A. T. P., Glover S. C. O., Klessen R. S., Clark P., 2021, MNRAS,
    507, 1775
Schleicher D. R. G., et al., 2022, MNRAS, 512, 6192
Scoggins M. T., Haiman Z., 2024, MNRAS, 531, 4584
Scoggins M. T., Haiman Z., Wise J. H., 2022, MNRAS, 519, 2155
Shang C., Bryan G. L., Haiman Z., 2010, MNRAS, 402, 1249
Tagawa H., Haiman Z., Kocsis B., 2020, ApJ, 892, 36
Tanaka T., Haiman Z., 2009, ApJ, 696, 1798
Tumlinson J., Shull J. M., 2000, ApJ, 528, L65
Vergara M. C., Escala A., Schleicher D. R. G., Reinoso B., 2022,
```

Global instability by runaway collisions in nuclear stellar clusters: Numerical tests of a route for massive black hole forma-

```
Volonteri M., 2010, The Astronomy and Astrophysics Review, 18, 279
Volonteri M., Lodato G., Natarajan P., 2008, MNRAS, 383, 1079
Volonteri M., Habouzit M., Colpi M., 2021, Nature Reviews Physics, 3, 732
Wang F., et al., 2021, ApJ, 908, 53
Wise J. H., Demchenko V. G., Halicek M. T., Norman M. L., Turk M. J., Abel T., Smith B. D., 2014, MNRAS, 442, 2560
Wise J. H., Regan J. A., O'Shea B. W., Norman M. L., Downes T. P., Xu H., 2019, Nature, 566, 85
Wolcott-Green J., Haiman Z., Bryan G. L., 2017, MNRAS, 469, 3329
Wu X.-B., et al., 2015, Nature, 518, 512
Yang X., et al., 2020, ApJ, 904, 200
```

tion, doi:10.48550/ARXIV.2209.15066, https://arxiv.org/abs/

2209.15066

This paper has been typeset from a TEX/LATEX file prepared by the author.